

A Constrained Genetic Approach for Reconstructing Young's Modulus of Elastic Objects from Boundary Displacement Measurements

Yong Zhang, Lawrence O. Hall, Dmitry B. Goldgof and Sudeep Sarkar
Department of Computer Science & Engineering
University of South Florida
Tampa, FL 33620
(zhang,hall,goldgof,sarkar)@csee.usf.edu

Abstract

This paper presents a constrained genetic approach (CGA) for reconstructing the Young's modulus of elastic objects. Qualitative a priori information is incorporated using a rank based scheme to constrain the admissible solutions. Balance between the fitness function (adhesion to the measurement data) and the penalty function (fidelity to a priori knowledge) is achieved by a stochastic sort algorithm. The over-smoothing of Young's modulus discontinuity is avoided without the need of computing a deterministic weight coefficient. The experiment on synthetic data indicates that the proposed method not only reconstructed reliable Young's modulus from noisy data, but also expedited the convergence process significantly.

1 Introduction

Elastography is a noninvasive technique for imaging elastic properties (Young's modulus) of soft objects. This technique is of interest to physicians for its potentials in early cancer detection and burn scar assessment [2, 12]. Reconstructing Young's modulus is also important for physics based modeling in computer graphics and vision [5, 10], because modeling results are strongly affected by the accuracy of material properties being used.

We can reconstruct the Young's modulus of an object by measuring its elastic deformation subject to external forces. Because of the ill-posed nature of this inverse problem [7] we have to use *a priori* knowledge to constrain the system so that an optimal and stable solution can be found.

Several important issues must be addressed for a reconstruction problem: (1) How the *a priori* information is incorporated? (2) How the contributions from measurement data and *a priori* information is balanced? (4) What method is used to solve the constrained minimization equation?

We propose to use a constrained genetic algorithm (CGA) to reconstruct the Young's modulus as a distributed parameter. This approach has the following features:

(1) *a priori* knowledge is incorporated through a rank table, which enables us to handle the qualitative information that can not be readily expressed as a continuous function and its derivatives. This kind of information about the object's properties can be collected from either experts (visual examination) or low level image processing.

(2) The balance between the fitness function (measurement data) and the penalty function (*a priori* knowledge) is achieved through stochastic ranking rather than by computing a deterministic weight coefficient.

(3) Reconstruction problems are often solved in a deterministic way, where the use of gradient based methods are common [1]. Kallel and Bertrand conducted experiments on elastic model using standard Newton-Raphson method [4]. In a previous study [12, 14], we used a steepest descent search to identify abnormal Young's modulus for burn scar assessment. The common drawback of the gradient based methods is that they are very sensitive to the starting point and hence often stuck in local minimum. This is very true when highly nonlinear physical models are used which results in an extremely complex solution space that is characterized by many local minima.

Recently, solving inverse problems in stochastic domains (global optimization) has received much attention. The stochastic nature of the genetic algorithm offers us a better chance to find a more optimal solution by escaping local minima. Wong and Guan [13] used evolutionary programming to solve an adaptively regularized image restoration problem. In electrical impedance tomography, Olmi *et al* [6] reported that a genetic algorithm is superior to the Newton-Raphson method in terms of the reconstruction accuracy. In this study, we demonstrate that it is possible to reconstruct the Young's modulus using a CGA and the strict requirement on starting point can be relaxed.

2 Finite Element Formulation of Young's Modulus Reconstruction

The elastic behavior of the body being acted upon by forces can be stated as a initial-boundary value problem:

$$\nabla \cdot (\mathbf{D}\mathbf{e}) + \rho\mathbf{f} = \rho \frac{\partial^2 \mathbf{u}}{\partial t^2} \quad (1)$$

where \mathbf{e} is strain tensor, \mathbf{D} is a matrix that includes Young's modulus (\mathbf{E}) to be recovered, \mathbf{u} is a displacement vector, ρ is the mass density, and \mathbf{f} is a force vector. \mathbf{D} also includes Poisson's ratio, which is assumed as a constant (0.495) in this study because of the small compressibility of soft tissues.

To solve (1), we transform it into a matrix equation using Galerkin method [15]:

$$\mathbf{M}\ddot{\mathbf{u}} + \mathbf{C}\dot{\mathbf{u}} + \mathbf{K}\mathbf{u} = \mathbf{F}(t) \quad (2)$$

where \mathbf{M} is the mass matrix, \mathbf{C} is the damping matrix, and \mathbf{K} is the stiffness matrix. In our study, (2) is simplified to the static case:

$$\mathbf{K}\mathbf{u} = \mathbf{F} \quad (3)$$

We reformulate (3) into:

$$\mathbf{A}(\mathbf{E}) = \mathbf{b} \quad (4)$$

where \mathbf{b} denotes boundary specifications (Dirichlet and Neumann) including displacement measurements, and \mathbf{A} is an operator that represents the forward physical model. \mathbf{A} is usually nonlinear and can be linearized using the perturbation method.

Because of the discontinuous dependence of \mathbf{E} on \mathbf{b} , the standard least square method in the form of $\min \|\mathbf{A}\mathbf{E} - \mathbf{b}\|$ can not guarantee a stable and optimal solution. The situation gets worse when vector \mathbf{E} has more components than \mathbf{b} does. *A priori* knowledge is therefore needed to constrain the least square solution:

$$\mathbf{E} = \arg.\min[L_1(\mathbf{A}\mathbf{E}, \mathbf{b}) + \beta L_2(\mathbf{E}, \mathbf{E}_{prior})] \quad (5)$$

where L_1 measures the fidelity of the solution $\mathbf{A}\mathbf{E}$ to data \mathbf{b} , L_2 denotes the distance between the computed solution \mathbf{E} and the expected solution \mathbf{E}_{prior} defining *a priori* knowledge on \mathbf{E} .

3 Constrained Genetic Algorithm

3.1 Genetic Encoding

We interpret the Young's modulus of finite element model as a chromosome in a CGA through a one-to-one

Finite Element Mesh
 $\mathbf{E}(i) = \text{Young's modulus of the } i\text{th element}$

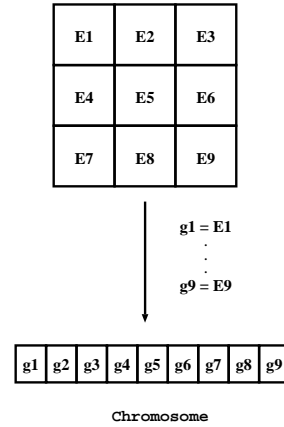


Figure 1. Genetic coding of Young's modulus in a finite element model

mapping between element and gene (Figure 1). So, if the finite element mesh has N elements, the corresponding chromosome has N genes. Each chromosome in the population pool represents a possible Young's modulus distribution. Because Young's modulus has continuous values, we use real-valued encoding (double) instead of a string of bits.

3.2 Rank Based Constraint

In the stochastic framework of genetic algorithms, the ill-posedness exhibits itself as local plateaus in the landscape of admissible solution space. Genetic algorithms are more stable in the sense that it can always converge to a solution, even though it may not be optimal. Constraints are imposed on solutions through penalty functions, which are equivalent to the regularization stabilizers or preconditioners in the deterministic framework.

We formulate the objective function to be minimized by a CGA as a combination of the fitness function and the penalty function:

$$obj(\mathbf{E}) = \|\mathbf{A}(\mathbf{E}) - \mathbf{d}\|_n^2 + wP(\mathbf{E}) \quad (6)$$

Where $\mathbf{A}(\mathbf{E})$ is displacement from finite element model, \mathbf{d} is the measured displacement vector, n is the number of nodes on which the measurement is made, $P(\mathbf{E})$ is a penalty function, and w is a weight coefficient (regularization parameter).

Like in the problem of spline and surface fitting, Young's modulus can be regarded as a spatial function $\mathbf{E}(\mathbf{x})$ that possesses a certain degree of continuity and therefore the smoothness constraint imposed on the surface of $\mathbf{E}(\mathbf{x})$ can be formulated as a quadratic integral functional:

$\int_{\mathbf{R}} |\Delta \mathbf{E}(\mathbf{x})|^2 d\mathbf{x}$ where Δ is the Laplace operator. One of the problems with this global smoothness constraint is that it might overdamp the discontinuity of Young's modulus commonly observed at the boundary of abnormal areas on the order of several magnitude in our burn scar study [12]). Various adaptive regularization schemes have been proposed to accommodate the local discontinuity [11, 3, 1].

Since we usually have good qualitative knowledge about the relative \mathbf{E} from a medical expert's assessment, or from low level image cues such as intensity gradient, color and texture, we propose an alternative rank based method to compute the penalty function. In each solution (chromosome), elements (genes) are ranked based on their relative Young's modulus and recorded in a sorted rank table. Similarly, we transform the qualitative *a priori* knowledge into another rank table. For each element, we compute the difference of its rank positions in two rank tables. We then sum up the rank discrepancy of all elements to represents the distance between the solution and *a priori* knowledge:

$$P(\mathbf{E}) = \sum_{i=1}^m \| r_i - R_i \|^2 \quad (7)$$

where r_i is the rank position of element i in the rank table of solution \mathbf{E} . R_i is the rank position of element i in the rank table of *a priori* knowledge.

Figure 2 illustrates the ranking scheme using a simple two-dimensional model of 4 elements. As *a priori* knowledge, the Young's modulus of each element is labeled as "high", "mid" and "low". This qualitative information is then transformed into a rank table where elements are sorted in descending order. If n elements ($n > 1$) have the same label, then they all can have n potential rank positions, which will be determined by its counterpart in the solution rank table. For instance, both element (1) and element (4) are labeled as "low", therefore their rank position can be 3 or 4. In solution 1, the ranks of element (2) and element (3) match exactly with their ranks in the table of *a priori* knowledge. For element (1), its rank in the solution table is 3, while its rank in *a priori* table is [3,4]. In the case of multiple ranks, we select the value that is closest to its counterpart in the solution table, which is 3 for element (1). Similarly, for element (4), we select 4 from its multiple *a priori* rank [3,4]. The final penalty value is zero ($P(\mathbf{E}) = 0$). In contrast, solution 2 has a \mathbf{E} distribution that is different from *a priori* knowledge and thus a shuffled rank table, which leads to a higher penalty value of 6.

We also introduce another penalty function that specifies the maximum and minimum Young's modulus an element could have. This upper bound and lower bound can be obtained either from literature or from *in situ* measurement.

This rank based approach has the advantage that it is intrinsically piecewise and thus preserves the parameter discontinuity (although a strong smoothness constraint can still

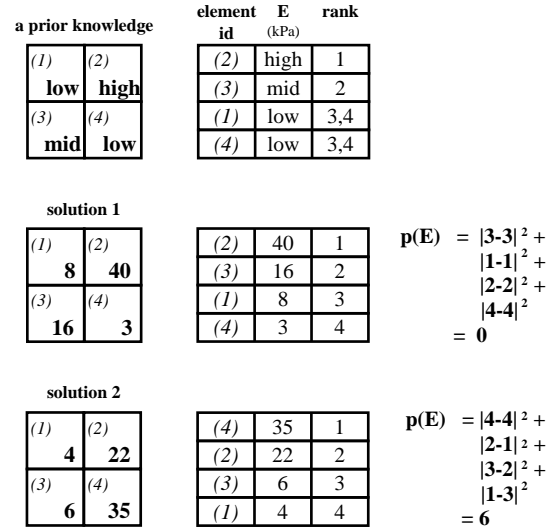


Figure 2. The rank based scheme for incorporating qualitative *a priori* information. The numbers in the parentheses denotes element ID and the bold numbers at the lower-left corner of elements represent Young's modulus (kPa).

be imposed in areas of little \mathbf{E} variations). This approach is particularly suitable for image based medical diagnosis such as scar assessment, where we are only interested in identifying and quantifying abnormal areas. Qualitative *a priori* knowledge can be collected by physicians who isolate and rate the scars. More automatic methods for extracting qualitative information from intensity gradient, texture and color are currently under investigation.

3.3 Balancing Fitness and Penalty Functions by Stochastic Ranking

In the objective function (6), the fitness function and the penalty function are computed on different quantities (fitness is measured as difference of displacement (m), while penalty function is the difference of rank orders (unitless)). An optimal weight coefficient w is needed to balance the contributions from the fitness and penalty functions. w is often problem dependent and finding an optimal w deterministically is still an open topic. In [8], Runarsson and Yao presented a stochastic method to strike a balance between two functions, without the need for computing w . We found this method is well suited for the problem of reconstructing Young's modulus by CGAs. Interested readers are referred to [8] for details.

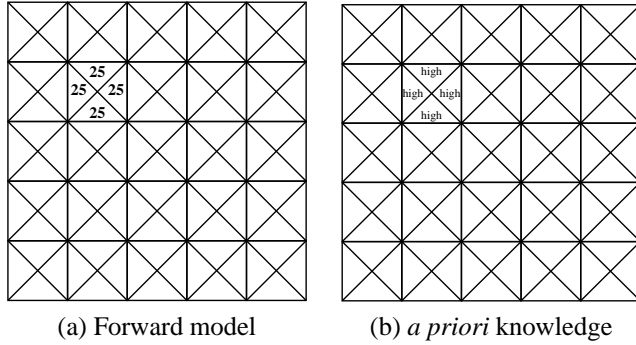


Figure 3. The forward finite element model and a priori knowledge. In (a), the Young's modulus of the background area is 5 (kPa). In (b), the background area is labeled as "low".

3.4 Other Genetic Operators

To minimize the objective function using a CGA, we specify several important genetic operators. We use a standard Gaussian mutation operator:

$$E_i^* = E_i + \sigma N(0, 1) \quad (8)$$

where E_i is the value of gene i before mutation, E_i^* is the value of gene i after mutation, $N(0, 1)$ is a random Gaussian number, and σ is the mutation step. The mutation step is determined by a predefined decay rate τ as: $\sigma(t) = \tau\sigma(t-1)$, where t is a generation counter. τ is usually set at the range of (0.9, 1.0). We experimented with dynamic setting of mutation probability (P_m) using population statistics and did not find significant improvement. So we set P_m to a fixed value of 0.5. The relatively high mutation rate is used to maintain the population diversity and prevent premature convergence. We also found that one-point crossover and multiple-point crossover perform equally well, at least in this particular problem. The crossover probability (P_c) is fixed to 0.7. Both parent selection and replacement operators are implemented as tournament selection ($k=2$) with an elitism strategy enabled (elite ratio is set to 10% of the population size).

4 EXPERIMENTAL RESULTS

4.1 Model Setup

We used a synthetic forward model to generate noise-free displacements with a predefined Young's modulus. The forward model was a two dimensional thin plate (10 cm by 10 cm) and was discretized to 61 nodes and 100 triangle elements (Figure 3 (a)). We chose a small square in the upper-left corner as the abnormal area with high Young's modulus

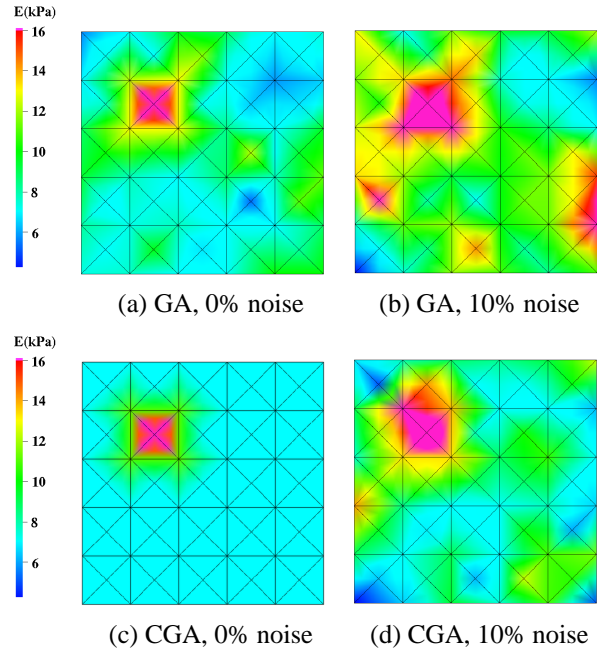


Figure 4. Reconstructed Young's modulus by GA and CGA. Note: the original figures are plotted in color. On the color scale, red and blue indicate high and low Young's modulus value, respectively. On grayscale print, most of the darker isolated areas have higher Young's modulus values.

value (25 kPa). The abnormal area includes 4 triangle elements (element ID: 23, 24, 71, 72). We set the Young's modulus in the rest of domain to be 5 kPa. We added forces at the boundaries to generate noise-free displacements. We then run both GA and CGA on those noise-free data to study to what degree the Young's modulus in the abnormal area can be reproduced. As our a priori knowledge, the four elements in the square were identified as a potential abnormal area. We labeled the four elements as "high" and other elements as "low" (Figure 3 (b)). To test the proposed method against noisy data, we added 10% white noise to the noise-free data. The experiments were performed on both noisy and noise-free data for comparison. We used Gaussian distribution as the initial guess of \mathbf{E} . For this 2D experiment, we found that a population size of 30 is large enough for the algorithm to converge to a good solution with less than 300 generations. For more complex 3D problems, an increase in population size and generation number might be necessary.

4.2 Performance Analysis

The performance of the proposed method is evaluated based on the reconstructed shape and Young's modulus value of the abnormal area as well as the convergence rate.

Table 1. Constructed E (kPa) in abnormal area

Element ID	True E	(a)	(b)	(c)	(d)
23	25	15.3	17.8	24.7	18.6
24	25	17.6	12.3	20.8	17.2
71	25	20.8	19.4	18.5	23.9
72	25	15.9	16.1	24.9	21.3
average	25	17.4	16.4	22.2	20.3

(a) GA, 0% Gaussian noise on measurement data. (b) GA, 10% noise. (c) CGA, 0% noise. (d) CGA, 10% noise.

For each test case, we run 10 experiments and therefore the conclusions are drawn from the average of 10 runs.

The constructed Young's modulus are shown in Figure 4. Given noise-free data, both GA and CGA can find the abnormal area with the boundary well defined. For noise corrupted data, the CGA (with good *a priori* knowledge) still successfully isolates the abnormal area although the boundaries are blurred, while the GA failed to find an acceptable solution as evidenced by the multiple abnormal areas that do not exist in the forward model.

The reconstructed Young's modulus of the abnormal area is summarized in Table 1. As expected, results from the CGA are more accurate than those from the GA.

The minimization processes are plotted in Figure 5. It is clear that the CGA outperforms the GA by reaching the same error level with much less generations. Of course, this convergence expedition is meaningful only if good *a priori* knowledge is used.

Although CGA is a computationally intensive method, it has a very desirable feature of being not sensitive to the initial condition (we used a Gaussian distribution as initial guess in all the experiments). In our previous study using gradient based methods, starting points that are away from the true solution often cause the algorithm to converge to a local minimum or simply diverge. A hybrid scheme is an attractive option where CGAs provide a good initial global approximation, upon which more efficient local gradient methods can be applied [9]. It should be noted that the forward model used to compute the fitness function is usually the bottleneck of the optimization process. In our experiments conducted on Sun Sparc ultra 5 (248 MHz, 2560 Mb), each run took about 12 hours, of which 95% of the time was consumed by the forward model.

5 SUMMARY

We present a constrained genetic approach for reconstructing the Young's modulus of elastic object under deformation. This approach utilizes a rank based mechanism to incorporate *a priori knowledge* to constrain the admissi-

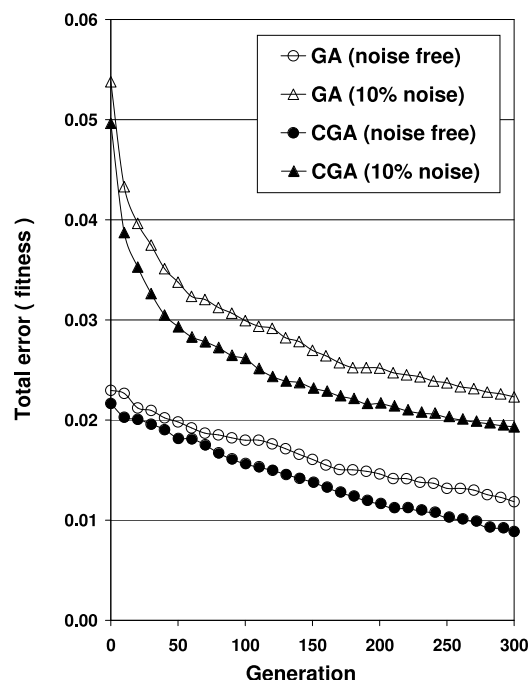


Figure 5. The convergence behavior of GA and CGA against noisy and noise-free data.

ble solutions. Experiments with noisy data indicate that the Young's modulus can be successfully recovered and significant improvements in both convergence rate and reconstruction accuracy have been observed.

References

- [1] H. W. Engl, M. Hanke, and A. Neubauer, "Regularization of inverse problems" Kluwer Academic Publishers, c1996.
- [2] J. B. Fowlkes, S. Y. Yemelyanov, J. G. Pipe, P. L. Carson, R. S. Adler, A. P. Sarvazyan, and A. R. Skovoroda, "Possibility of cancer detection by means of measurement of elastic properties" *Radiology*, Vol. 185, pp. 206-207, 1992.
- [3] C. R. Johnson, R. S. MacLeod, "Local Regularization and Adaptive Methods for the Inverse Laplace Problem," *Biomedical and Life Physics*, Vieweg-Verlag, pp. 224-234, 1996.
- [4] F. Kallel and M. Bertrand, "Tissue elasticity reconstruction using linear perturbation method" *IEEE Transactions on Medical Imaging*, 15(3), pp. 299-313, 1996.
- [5] R. M. Koch, M. H. Gross, F. R. Carls, D. F. von Buren, G. Fankhauser, and Y. I. H. Parish, "Simulating Facial Surgery Using Finite Element Models," *Proceedings of SIGGRAPH's 96*, pp. 421-428, 1996.
- [6] R. Olmi, M. Bini and S. Priori, "A genetic algorithm approach to image reconstruction in electrical impedance tomography" *IEEE Transactions on Evolutionary Computation*, Vol. 4, No. 1, pp. 83-88, 2000.
- [7] K. R. Raghavan and A. Yagle, "Forward and inverse problems in imaging the elasticity of soft tissue" *IEEE Transactions on Nuclear Science*, 41(4), pp. 1639-1647, 1994.

- [8] T. P. Runarsson and X. Yao, "Stochastic ranking of constrained evolutionary optimization" *IEEE Transactions on Evolutionary Computation* , Vol. 4, No. 3, pp. 284-294, 2000.
- [9] R. Salomon, "Evolutionary algorithms and gradient search: Similarities and differences" *IEEE Transactions on Evolutionary Computation* , Vol. 2, No. 2, pp. 45-55, 1998.
- [10] D. Terzopoulos, and K. Waters, "Analysis and synthesis of facial image sequences using physical and anatomical models," *IEEE Transaction on Pattern Analysis and Machine Intelligence*, 15(6), pp. 569-579, 1993.
- [11] D. Terzopoulos, "Regularization of visual problems involving discontinuities," *IEEE Transaction on Pattern Analysis and Machine Intelligence*, Vol. 8, pp. 413-424, 1986.
- [12] L. V. Tsap, D. B. Goldgof, S. Sarkar and P. S. Powers, "A vision-based technique for objective assessment of burn scars" *IEEE Transactions on Medical Imaging*, 17(4), pp. 620-633, 1998.
- [13] H. Wong and L. Guan, "Application of evolutionary programming to adaptive regularization in image restoration" *IEEE Transactions on Evolutionary Computation* , Vol. 4, No. 4, pp. 309-326, 2000.
- [14] Y. Zhang, D. B. Goldgof, S. Sarkar and L. V. Tsap, "Model-based nonrigid motion analysis using natural feature adaptive mesh," *Proceedings of International Conference on Pattern Recognition*, pp. 839-843, 2000.
- [15] O. C. Zienkiewicz, "The Finite Element Method," 3rd edn, McGraw-Hill, 1977.